

Supplementary Materials

Silica diagenesis promotes early primary hydrocarbon migration

Israa S. Abu-Mahfouz^{1*}, Joe Cartwright¹, Erdem Idiz¹, John N. Hooker², and Stuart A. Robinson¹

¹ *Department of Earth Sciences, University of Oxford, South Parks Road, Oxford, OX1 3 AN, UK*

² *Department of Geosciences, The Pennsylvania State University, 503 Deike Bldg., University Park, PA 16802, USA*

**i_abumahfouz85@yahoo.com*

SUMMARY

This supplementary material includes a summary of the methods used in this study (Table DR1), and TOC data of the analysed reaction rims and their host mudstone (Table DR2).

It also includes a schematic E-W cross section of Jordan (Fig. DR1), a histogram showing the distance from the reaction rim to the nearest bitumen vein (Fig. DR2), photomicrographs showing the change in bitumen distribution and the main minerals from the centre of the chert nodule outwards (Fig. DR3), Photomicrographs of the three zones (chert nodule, reaction rim and Host mudstone), showing a range of features observed (Fig. DR4), a BSE image and EDS maps showing the composition of the chert nodule, reaction rim and host mudstone (Fig. DR5), and a histogram showing the compositions of the chert Nodule, reaction rims and host mudstones, calculated from EDS maps (Fig. DR6). Figure DR7 presents A 'cartoon-like' diagram showing the evolution of the concretions, bitumen filaments and bitumen veins. From precursor host sediment of siliceous (biogenic), organic-rich mudstone, to concretion formation, to reaction rim and fracturing/bitumen migration.

Table DR1. The methods and equipment used to conduct the current study.

Analysis	Equipment used
<p>Samples were pulverized, weighed and analysed for their Total Organic Carbon (TOC) in order to measure their organic carbon fractions. TOC was examined for pair samples from host mudstone and related reaction rims.</p>	<p>A Vinci Technologies (Nanterre, France) Rock-Eval VI was used for this analysis. Long-term reproducibility of TOC values of external and internal standards is typically better than $\pm 0.4\%$</p>
<p>Thin sections with a thickness of 30 μm were prepared from samples collected in systematic transects from the organic-rich mudstone across the nodule reaction rims and into the chert nodules in order to compare textures and compositions along these transects. All SEM analyses were performed at 20 kV and a working distance of about 10 mm.</p>	<p>Optical analyses of thin sections were performed in cross-polarized light with a Nikon Optophot Microscope linked with a digital camera.</p> <p>The thin sections were also examined using a FEI Quanta 650 FEG scanning electron microscope (SEM). Backscattered electron (BSE) images were created to study mineral compositions and textures of the samples. Elemental mapping was performed using an energy-dispersive X-ray spectroscopy (EDS) attachment to the SEM.</p>

Table DR2. TOC data of the analysed reaction rims and their host mudstone

Blob Number	Reaction Rim (TOC, wt%)	Host Mudstone (TOC, wt%)
B1	4.88	11.94
B2	5.28	12.06
B3	11.88	17.89
B4	4.6	13.32
B5	8.07	11.02
B6	6.98	13.26
B7	5.5	11.1
B8	5.4	17.4
B9	6.3	17.8

FIGURE CAPTIONS

Figure DR1. A schematic E-W cross section of Jordan. Modified from Alder, 1985. The cross section is outlined in Fig. 1 (red double arrow).

Figure DR2. Distance from the reaction rim to the nearest bitumen vein, measured from the Lower Unit of each of the study cores (for core locations see Figure 1a). BV, Bitumen Vein. N=84. Note that 94% of BVs are <4 mm away from the nearest reaction rim. 60% of the BVs are present within the reaction rim.

Figure DR3. A montage of photomicrographs across the transition zones (shown in yellow in the right schematic drawing) showing the change in bitumen (B) distribution and the main minerals from the centre of the chert nodule outwards. Note the development of the bitumen veins in the reaction rims. TZ1, Transition zone 1; TZ2, Transition Zone 2. MQz, Microcrystalline Quartz; G, Ghost of Fossil; BV, Bitumen Vein; Bit, Disseminated Bitumen; Chalc, Chalcedony.

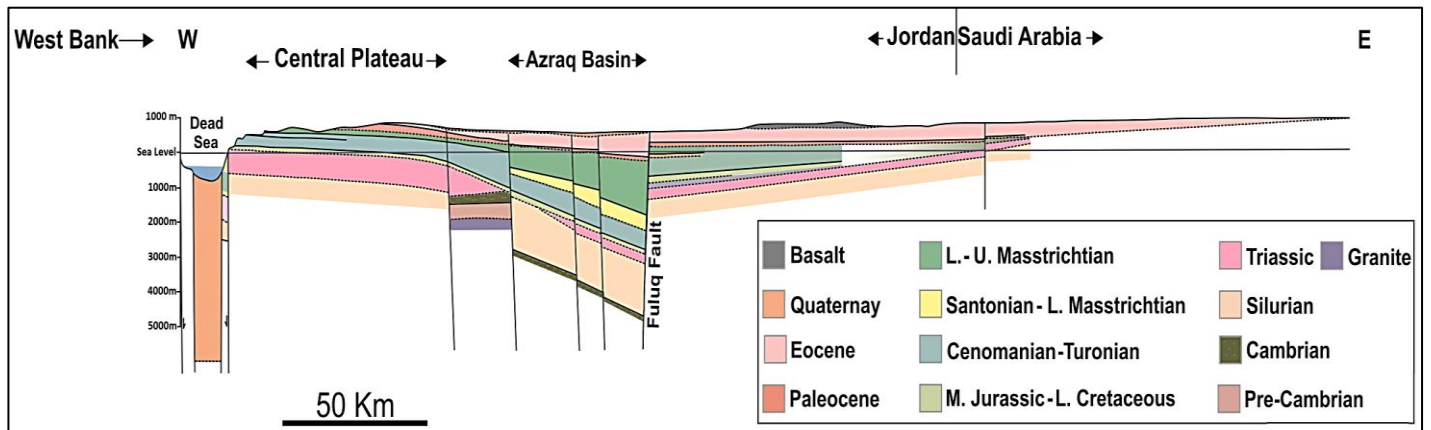
Figure DR4. Photomicrographs of the three zones, showing a range of features observed, including (A) Well-preserved (uncompacted) forams in the chert nodule; indicating early formation of the chert nodule. (B) Fossil ghosts (G) inside the chert nodule. (C-D) Transitional zone between the chert nodule and the reaction rims (RR). Note the development of bitumen veins in the RR. Note the decrease in the microcrystalline Qz fraction towards the RR. Scale bar is 1 mm.

Figure DR5. A BSE image and EDS maps showing the composition of the chert nodule, reaction rim and host mudstone (from the centre of the nodule (top) through the reaction rim (middle) to the mudstone (bottom)). Si, Silica; Ca, Calcium

Figure DR6. Compositions of the chert concretions (Chert Nodule.), reaction rims and host mudstones, calculated from EDS maps. C, Organic Carbon; K, Potassium.

Figure DR7. A 'cartoon-like' diagram showing (from I to IV) the evolution of the concretions, bitumen filaments and bitumen veins. From precursor host sediment of siliceous (biogenic), organic-rich mudstone, to concretion formation, to reaction rim and fracturing/bitumen migration.

Figure DR1



Alder, K., 1985, Jordan Regional Cross Section A-A': Occidental Exploration and Production Company.

Figure DR2

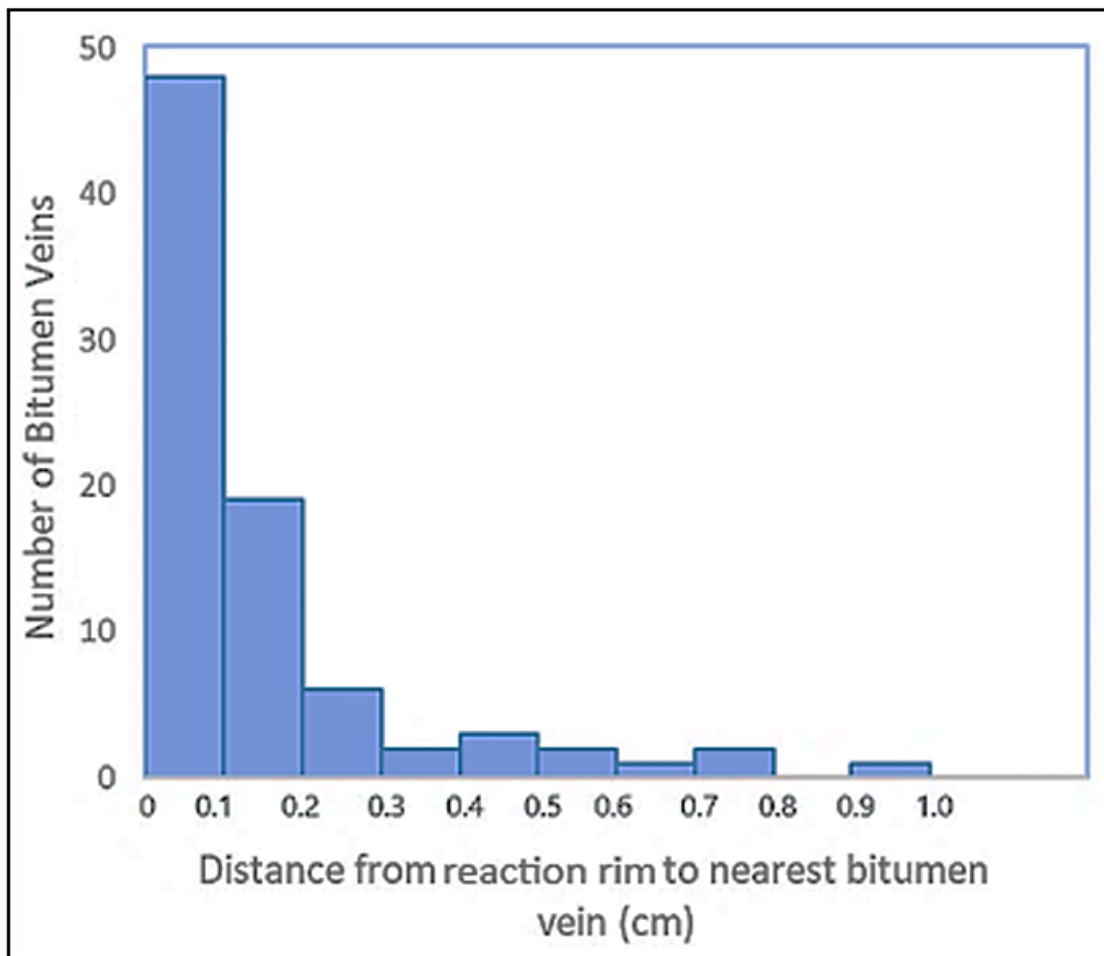


Figure DR3

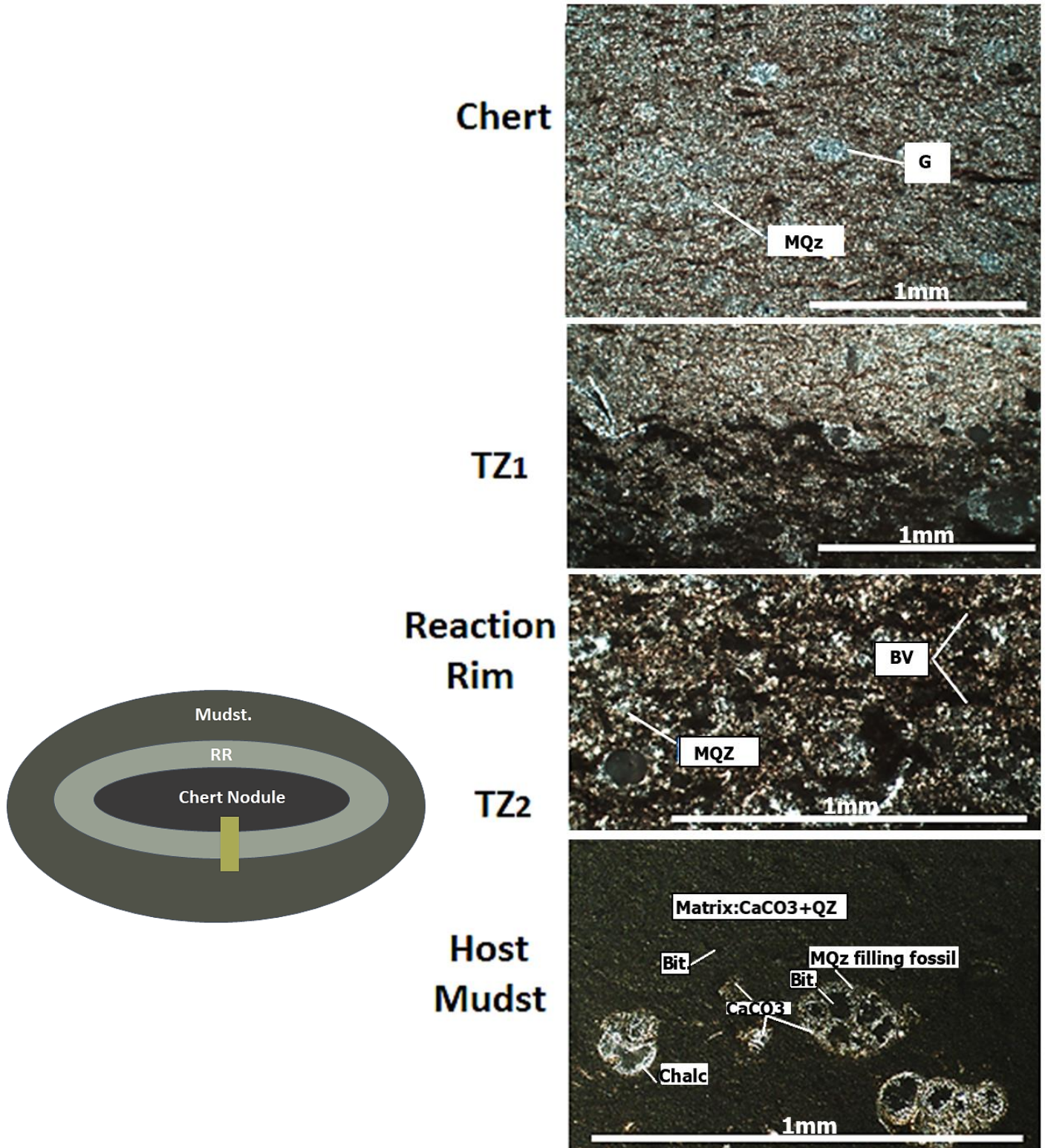


Figure DR4

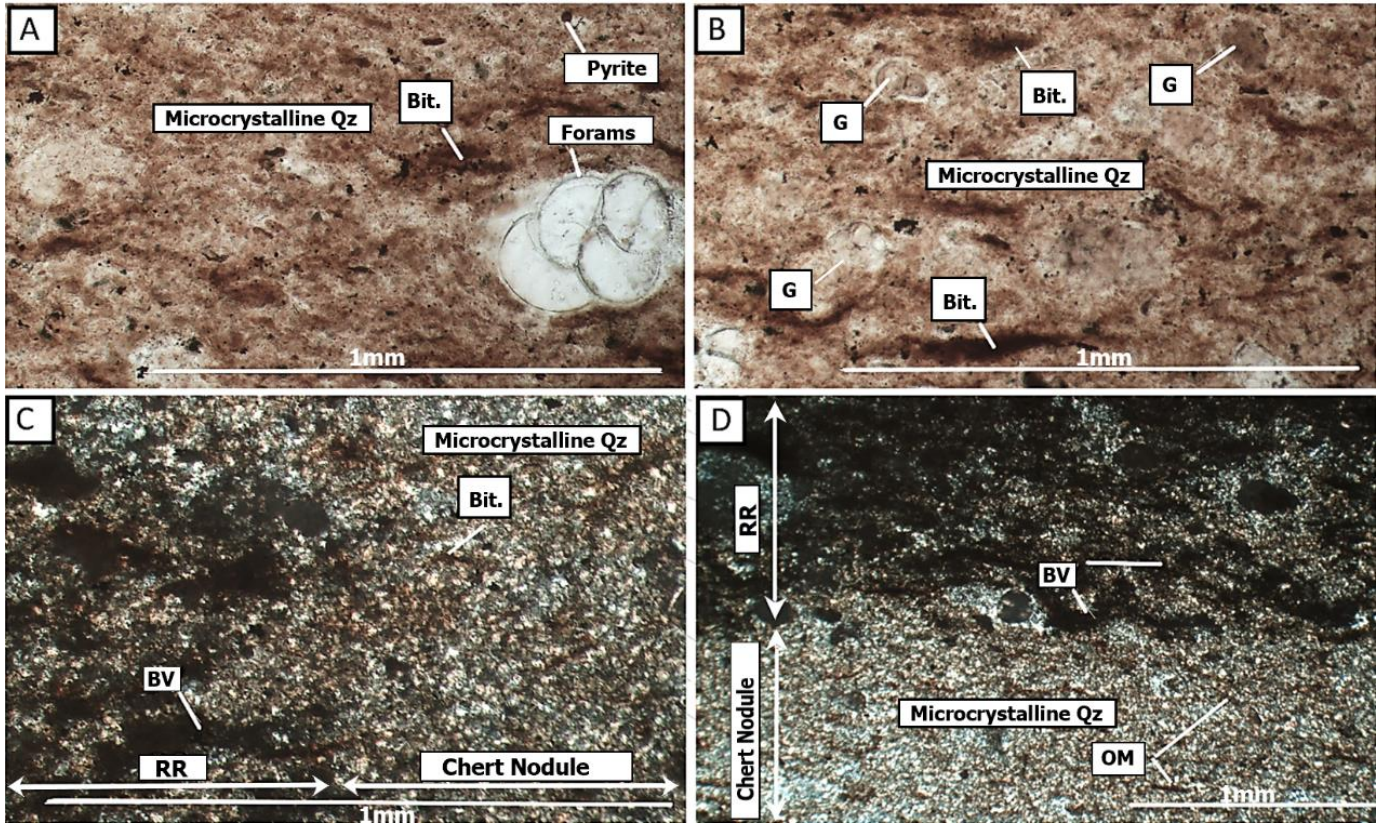


Figure DR5

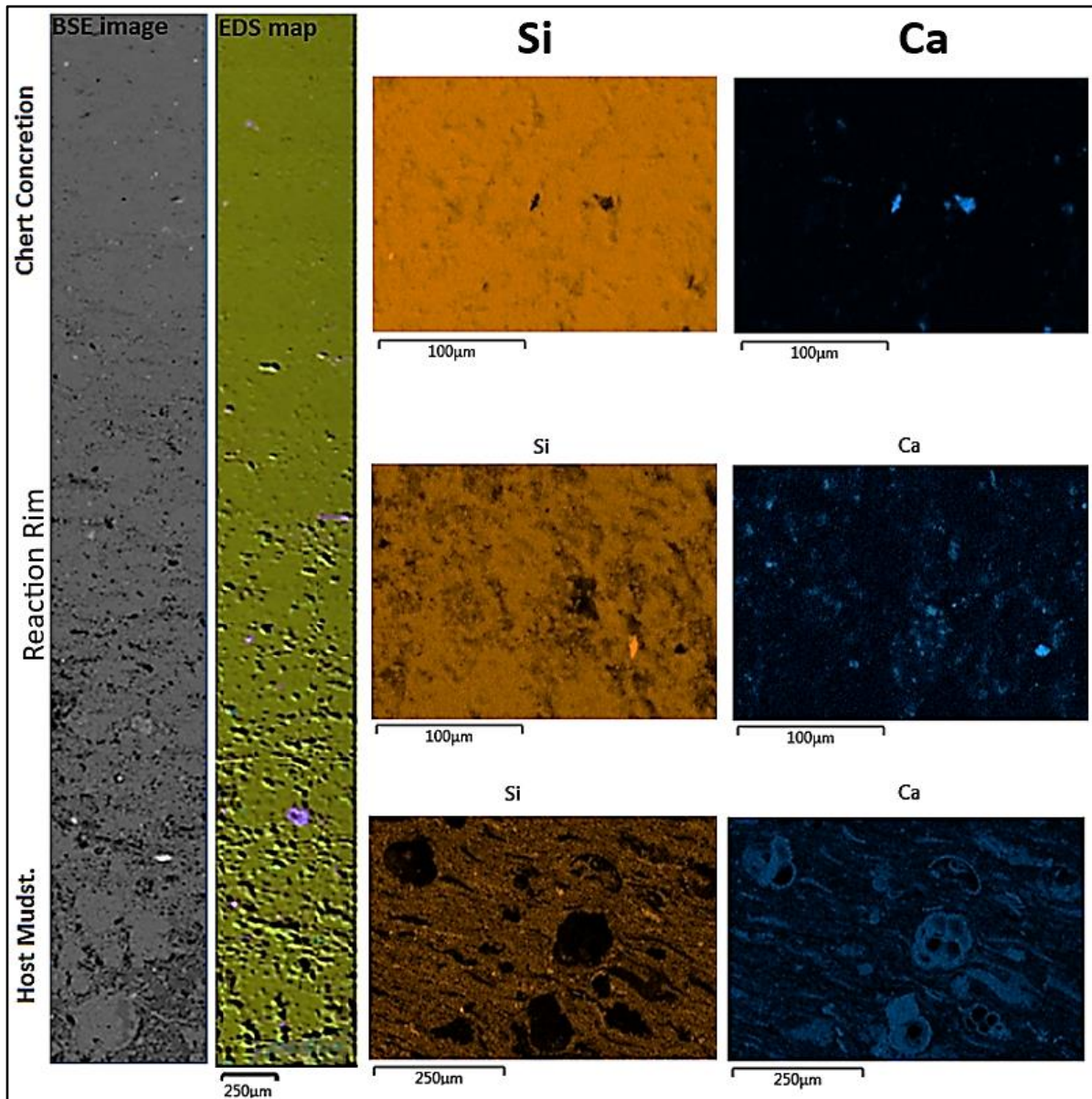


Figure DR6

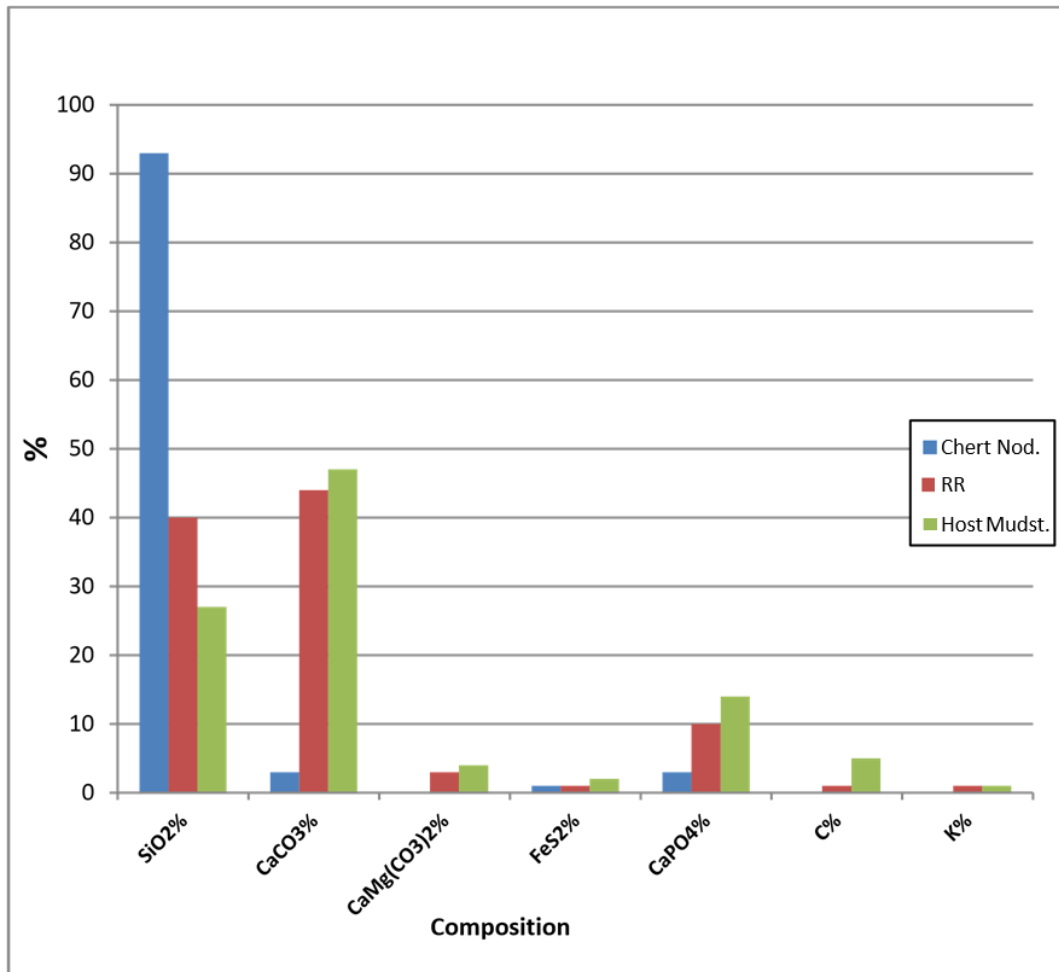


Figure DR7

